

Generation and Propagation of a Picosecond Acoustic Pulse at a Buried Interface: Time-Resolved X-Ray Diffraction Measurements

S. H. Lee,^{1,*} A. L. Cavalieri,^{1,†} D. M. Fritz,¹ M. C. Swan,¹ R. S. Hegde,² M. Reason,² R. S. Goldman,² and D. A. Reis¹

¹*FOCUS Center and Department of Physics, University of Michigan, Ann Arbor, Michigan 48109-1040, USA*

²*Department of Material Science & Engineering, University of Michigan, Ann Arbor, Michigan 48109-2136, USA*

(Received 29 August 2005; published 9 December 2005)

We report on the propagation of coherent acoustic wave packets in (001) surface oriented $\text{Al}_{0.3}\text{Ga}_{0.7}\text{As}/\text{GaAs}$ heterostructure, generated through localized femtosecond photoexcitation of the GaAs. Transient structural changes in both the substrate and film are measured with picosecond time-resolved x-ray diffraction. The data indicate an elastic response consisting of unipolar compression pulses of a few hundred picosecond duration traveling along $[001]$ and $[00\bar{1}]$ directions that are produced by predominately impulsive stress. The transmission and reflection of the strain pulses are in agreement with an acoustic mismatch model of the heterostructure and free-space interfaces.

DOI: [10.1103/PhysRevLett.95.246104](https://doi.org/10.1103/PhysRevLett.95.246104)

PACS numbers: 68.35.Iv, 61.10.-i, 68.60.-p, 78.47.+p

Thermal transport in nanoscale materials is a fundamental problem in condensed matter physics and is of great importance for development of practical devices [1]. Of particular importance at small length scales is the interfaces between materials. Phonons transfer heat between materials and their scattering is particularly sensitive to the details of the interface [2,3]. Early studies of phonon propagation across a superlattice used superconducting tunnel junctions as the phonon source and detector [4]. Recently, femtosecond lasers have found use in nanoscale thermal transport measurements, including all optical measurements of thermal conductivity [5,6] and thermal boundary resistance of solid-solid [7] and solid-liquid interfaces [8]. In these experiments the laser plays a dual role, both creating the phonons (coherent or incoherent) and detecting them indirectly through changes in the optical properties.

In contrast, x-ray techniques are able to yield quantitative information about the atomic positions. Time-resolved x-ray diffraction (TRXD) has proven a versatile probe to study bulk and surface lattice dynamics on picosecond and faster time scales. Recent x-ray experiments have included measurements of strain generation following short pulse laser excitation in metals [9] and semiconductors [10–14], phonon damping in thin Ge films [15] and phonon folding in multiple quantum wells [16,17].

In this Letter, we present novel experiments on the transport of a coherent acoustic wave-packet across the nearly ideal $\text{Al}_x\text{Ga}_{1-x}\text{As}/\text{GaAs}$ interface. A femtosecond laser impulsively excites the underlying substrate such that the coherent acoustic phonons take the form of two counterpropagating unipolar pulses. Picosecond TRXD is used to observe the laser-induced strain separately for the film and substrate. On the time scale of these experiments, the strain in the film is purely elastic because the carriers are confined in the substrate and thermal diffusion is slow compared to the sound propagation time across the film.

We observe the transmission and reflection of the acoustic pulse in the two extreme limits of a near perfect acoustic match between the film and the substrate and a near infinite acoustic mismatch between the film and the air. The x-ray data are in good agreement with numerical simulations of the strain generation and propagation assuming instantaneous stress and an acoustic mismatch model [2,4] for the two interfaces. These proof of principle experiments demonstrate that time-resolved x-ray diffraction can provide quantitative information on nanoscale thermal transport.

The experiments are performed at the MHATT-CAT Sector 7 time-resolved insertion device beam line at the Advanced Photon Source (APS), details of which have been described elsewhere [12,14,18]. The pump pulses are delivered from a kHz repetition rate, amplified ultrafast Ti:sapphire laser with circa 50 fs, 0.75 mJ pulses at a central wavelength of 800 nm. The x-ray probe from the undulator consists of a train of pulses that is monochromatized with a cryogenically cooled double crystal Si 111 monochromator. Active feedback of the Ti:sapphire oscillator cavity length maintains synchronization between the laser and x-ray pulses to better than 5 ps (rms), such that the temporal resolution is limited by the x-ray bunch duration, ~ 100 ps (FWHM). The pump-probe delay is set using a digital delay in the laser pulse selection to provide coarse timing over ± 1 ms, while a digital phase shifter provides fine tuning with 19 ps precision with no loss in resolution. The x-ray detector is an avalanche photodiode, and a boxcar integrator is used to select a single pulse at the repetition rate of the laser.

The sample consists of a single $1.5 \mu\text{m}$ thick (001) $\text{Al}_{0.3}\text{Ga}_{0.7}\text{As}$ layer grown on (001) bulk GaAs by molecular beam epitaxy and capped with a thin protective GaAs layer. This particular alloy was chosen to be transparent to the pump laser beam while having an excellent acoustic match with the substrate. It is this latter property that results in the unipolar compression wave that is launched from the bulk

into the film, as discussed below. The multilayer sample is oriented in the symmetric 004 Bragg geometry at room temperature for an x-ray energy of 10 keV. Although the lattice mismatch between the two materials is small, two distinct Bragg diffraction peaks are resolved, see Fig. 1. From the difference in the Bragg angles, the mismatch in lattice spacing along the growth direction is calculated to be 0.09%. The small modulation between the Bragg peaks are due to finite thickness effects in the film and interference between x rays diffracted from the wings of the $\text{Al}_{0.3}\text{Ga}_{0.7}\text{As}$ and GaAs rocking curves.

Laser pulses are incident on the airside of the $\text{Al}_{0.3}\text{Ga}_{0.7}\text{As}$ layer at a 1 kHz repetition rate. The laser photon energy, 1.55 eV, is significantly less than the electronic energy band gap of $\text{Al}_{0.3}\text{Ga}_{0.7}\text{As}$, 1.79 eV, such that the film is effectively transparent to the laser, and the photons are absorbed in the GaAs substrate with an absorption length of approximately $1\ \mu\text{m}$. The conduction band of the $\text{Al}_{0.3}\text{Ga}_{0.7}\text{As}$ is also sufficiently higher in energy than that of the GaAs such that the hot photoexcited carriers are confined to the GaAs. On a longer time scale, thermal transport across the boundary will heat the $\text{Al}_{0.3}\text{Ga}_{0.7}\text{As}$ as the GaAs cools. Since the x-ray Bragg peaks from the film and the substrate can be separately resolved, propagation of the laser-generated strain pulse and the temperature can be independently measured in the substrate and film.

We expect that the above-band-gap excitation in the GaAs by the ultrafast laser leads to the generation of a near instantaneous stress due to the creation and relaxation of a dense electron-hole plasma. The plasma is initially present only in a thin layer where the photoexcited carriers are generated. As the plasma diffuses and recombines, thermalizing with the lattice, strain is produced in the form of thermal expansion and an elastic response consisting of two counterpropagating compressive pulses. The thermalization process is fast and the plasma diffusion is slow compared with the acoustic transit time across the optical penetration depth, such that a simple thermoelastic

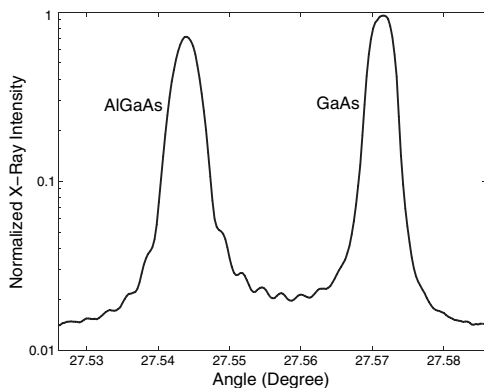


FIG. 1. Static x-ray diffraction trace from a single heterostructure sample consisting of a $1.5\ \mu\text{m}$ (001) $\text{Al}_{0.3}\text{Ga}_{0.7}\text{As}$ epitaxial film grown on (001) GaAs. The two individual 004 Bragg peaks are clearly resolved.

model describes the resultant strain [19]. For bulk materials, this model predicts a symmetric bipolar uniaxial strain pulse that propagate at the longitudinal speed of sound. One of the pulses immediately propagates into the bulk; the other propagates towards the free surface, becoming a tensile pulse following reflection. In the present case, the strain is modified by the existence of the $\text{Al}_{0.3}\text{Ga}_{0.7}\text{As}$ film which separates the free surface from the region of photoexcitation.

Since the frequency of the phonons associated with the strain is low compared to frequency of the x-ray probe, time-resolved diffraction can be considered in the quasi-elastic regime, where strain locally changes the Bragg angle at a time following photoexcitation [14]. Figure 2(a) shows a time scan of the diffraction at an angle of 27.546° , on the high angle side of the $\text{Al}_{0.3}\text{Ga}_{0.7}\text{As}$ Bragg peak. The initial increase in the diffraction intensity corresponds to shifting of the Bragg peak to a greater angle, and thus a decrease in lattice spacing due to the compressive pulse being launched from the GaAs substrate. Approximately 300 ps later, the leading edge of the strain pulse in the film arrives at the solid-air interface, and it reflects back toward the substrate side. During this process, a π phase shift is introduced in the strain pulse due to the effectively infinite acoustic impedance of the air, and it gives rise to a tensile reflected strain pulse. As a result, the compression pulse becomes an expansion pulse; the lattice spacing of the $\text{Al}_{0.3}\text{Ga}_{0.7}\text{As}$ layer increases and the Bragg peak shifts to smaller angles. This interpretation is supported by the subsequent decrease in the x-ray intensity on the high angle side of the Bragg peak as seen in Fig. 2(a). We can confirm this interpretation from the opposite behavior seen in the time-resolved diffraction

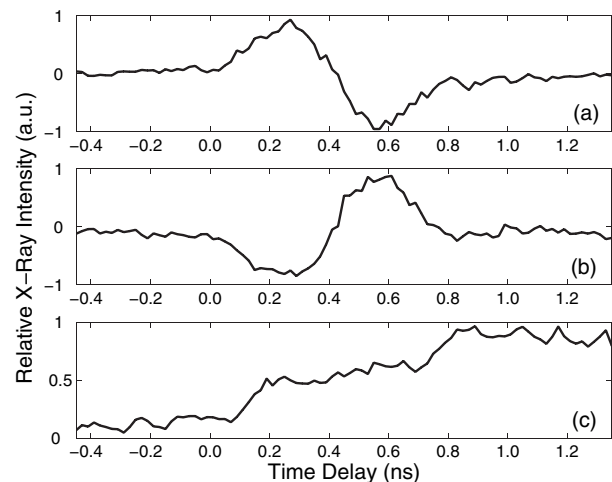


FIG. 2. Intensity of the x-ray diffraction (measured relative to before excitation and normalized to the maximum) following femtosecond laser excitation above the gap in the GaAs substrate. Three different angles near the 004 Bragg peak are shown: (a) 27.546° , on the high angle side of the $\text{Al}_{0.3}\text{Ga}_{0.7}\text{As}$ peak; (b) 27.5415° , on the low angle side of the $\text{Al}_{0.3}\text{Ga}_{0.7}\text{As}$ peak; and (c) 27.5690° , on the low angle side of the GaAs peak.

efficiency measured at an angle 27.5415° on the low angle side of the unperturbed $\text{Al}_{0.3}\text{Ga}_{0.7}\text{As}$ Bragg peak [Fig. 2(b)]. As the unipolar strain pulse is transmitted back into the GaAs substrate, the Bragg peak returns to its initial value, indicating that no significant thermal expansion due to heat transfer across the interface has occurred. Within the limits of our detection, we see no evidence of a partial reflection from the interface.

The acoustic propagation time across the film is measured to be about 300 ps and is consistent with propagation of the strain pulse at the longitudinal speed of sound (4955 m/s) and thickness of $1.5 \mu\text{m}$ $\text{Al}_{0.3}\text{Ga}_{0.7}\text{As}$ layer. In the present case, determination of the film thickness by the propagation time is limited by the temporal resolution, and to a lesser extent on the details of the strain profile. We note that the width of the pulse can be determined from the time delay between the peak and the zero crossing in the relative diffraction efficiency. At this precise instance, the integrated strain in the film is zero (equal amounts of compression and expansion). We estimate the pulse width of the strain to be $0.75 \mu\text{m}$, or $1.1 \mu\text{m}$ $1/e$ length assuming an exponential profile.

As the initial compressive strain pulses propagate away from the heated photoexcited region of the substrate layer, it leaves behind a region of thermal expansion, as can be seen from Fig. 2(c). The x-ray diffraction efficiency at 27.569° , on the low angle side of the unperturbed GaAs Bragg peak, increases with time as the strain pulse propagates out of the region of laser excitation. After approximately 600 ps, the component of the strain pulse that was launched into the $\text{Al}_{0.3}\text{Ga}_{0.7}\text{As}$ layer returns to the substrate as an expansive pulse. This results in a further increase in the local lattice spacing, as can be seen by the additional increase in x-ray diffraction (the amplitudes of thermal expansion and strain pulses add). In fact, the change in diffraction efficiency nearly doubles indicating that the nonacoustic component to the strain has not significantly evolved on the $\sim\text{ns}$ time scale. Not shown in the figure, the diffraction efficiency gradually decreases as the tensile strain travels deep into the bulk out of the x-ray probed region leaving the thermally expanded region behind to decay on the longer time scale of diffusion and carrier relaxation.

We modeled the strain profile to compare with the x-ray diffraction data. In our simulation, changes in atomic lattice spacing are obtained by calculating the total strain from bulk material based on the model of Thomsen *et al.* [19]. The strain is calculated from differential thermal expansion in which a changing temperature distribution gives rise to two compressive strain pulses that propagate in opposite directions. The calculated strain profiles are shown in Fig. 3 for four different delay times. Initially three different strain components are assigned to the GaAs substrate, two compressive strain waves that propagate with the longitudinal speed of sound in opposite directions and a region of expansive strain, that we approximate as static, as it diffuses into the crystal on the much longer time

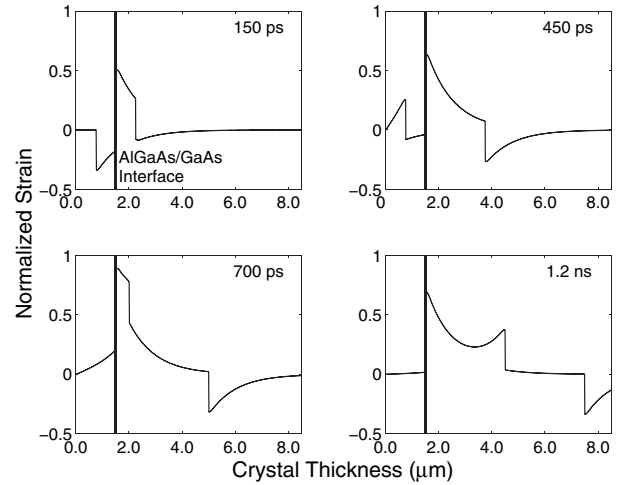


FIG. 3. Simulation of the strain as a function of depth at four different time delays following laser excitation where the energy is deposited in a thin region of the GaAs substrate. A simple thermoelastic model is used in which the strain is due to differential thermal expansion and diffusion is slow. An elastic response is generated which travels at the longitudinal speed of sound. The transmission coefficient for the pulse at the heterostructure interface is unity and the reflection coefficient at the free surface is -1 . Notice that a unipolar compression pulse propagates through the $\text{Al}_{0.3}\text{Ga}_{0.7}\text{As}$ film, reflects off the free surface becoming a tensile pulse, and later transmits into the GaAs substrate.

scale of thermal diffusion. We note that in GaAs, the lattice expands with increased carrier concentration, so as long as carrier diffusion and recombination are slow, the stress and subsequent strain due to carriers gives rise to a strain with the same spatial profile as given by thermal expansion. In fact, for near gap excitation to the Γ valley, we expect the volume deformation potential to provide for the dominant stress.

The propagating strain pulse consists primarily of long-wavelength acoustic phonons, limited by the laser penetration depth in the bulk, and on order of the thickness of the film. The transmission across the solid-solid interface is calculated in the acoustic mismatch limit [2] to be $t = 0.995$, so that in this limit reflections are expected to be negligible. Since the GaAs protective layer is thin compared to the phonon wavelength, the free surface of the film is taken as $\text{Al}_{0.3}\text{Ga}_{0.7}\text{As}$ -vacuum interface, which results in a near perfect reflection of the compressive strain accompanied by a π phase shift.

Figure 4 shows data and simulation of a time and angle scan about the 004 $\text{Al}_{0.3}\text{Ga}_{0.7}\text{As}$ peak. The glitches in the data at approximately 0.2 and 0.6 ns are due to the periodic topping off of the electron bunch charge in the storage ring and thus a rise in average x-ray flux. From the shift in the Bragg peak, we estimate the maximum strain in the $\text{Al}_{0.3}\text{Ga}_{0.7}\text{As}$ film to be $\sim 2 \times 10^{-5}$. The data is modeled using dynamical theory of x-ray diffraction [20] modified to incorporate strain [21,22]. The simulation using the

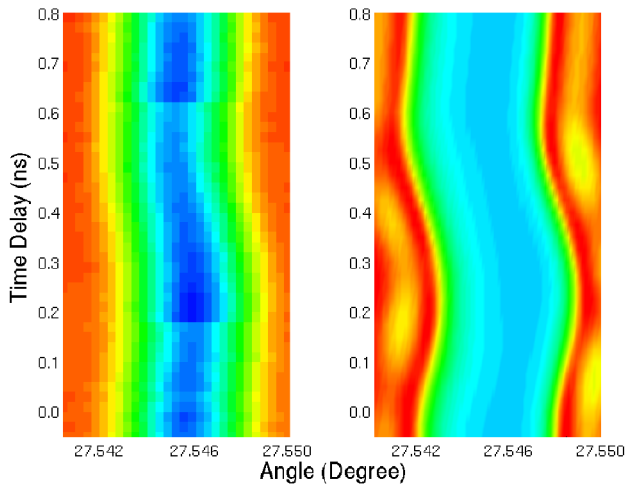


FIG. 4 (color online). Time and angle resolved x-ray diffraction from the $\text{Al}_{0.3}\text{Ga}_{0.7}\text{As}$ film showing the propagation of a short acoustic pulse that was generated in the GaAs substrate. Experimental data are on the left and a simulation in which strain is incorporated into dynamical diffraction theory is on the right.

strain profiles shown in Fig. 3 reproduces the behavior seen in the data indicating that strain is well described by the generation of an instantaneous stress in the substrate and a very small acoustic mismatch at the heterostructure interface.

In conclusion, we have measured the propagation of a unipolar coherent acoustic pulse in a single epitaxial $\text{Al}_{0.3}\text{Ga}_{0.7}\text{As}/\text{GaAs}$ heterostructure using time-resolved x-ray diffraction. The data are in agreement with a strain profile that is produced predominantly by impulsive stress. The pulse, with micron-scale spatial extent, is generated by femtosecond laser-absorption in a thin region on the substrate side of the interface. The transmission of the pulse across the interface is consistent with an acoustic mismatch model for long-wavelength phonons with a near perfect acoustic impedance match, while reflection at the free surface agrees with an infinite acoustic mismatch. In addition to providing further insight into the strain generation process, the added specificity of x-ray diffraction combined with the ability to measure phonons at a given wave vector, as well as measure the local temperature, should prove a useful tool in measuring frequency dependent thermal and mechanical properties of thin films and interfaces. These experiments could be extended to large wavevectors, for example by generating short wavelength coherent phonons in multiple quantum wells or metallic films. Ultimately time-resolved diffuse scattering [23] can yield complete phonon dynamics throughout the entire Brillouin zone.

We thank Dohn Arms, Eric Dufresne, Eric Landahl, and Dohn Walko for experimental assistance and Stephen Fahy and Roberto Merlin for useful discussions. This work was conducted at the MHATT-CAT insertion device beam line at the Advanced Photon Source and was supported in part

by the U.S. Department of Energy, Grants No. DE-FG02-00ER1503, and from the NSF FOCUS physics frontier center. M. R. and R. S. G. acknowledge the support of the DoD Multidisciplinary University Research Initiative administered by the Air Force Office of Scientific Research under Grant No. F49620-00-1-0328. Use of the Advanced Photon Source was supported by the U.S. Department of Energy, Office of Science, Office of Basic Energy Sciences, under Contract No. W-31-109-Eng-38.

*Electronic address: shl@umich.edu

†Present address: Max-Planck-Institute of Quantum Optics Hans-Kopfermann-Str. 1 D-85748 Garching, Germany.

- [1] D. G. Cahill, W. K. Ford, K. E. Goodson, G. D. Mahan, A. Majumdar, H. J. Maris, R. Merlin, and S. R. Phillpot, *J. Appl. Phys.* **93**, 793 (2003).
- [2] E. T. Swartz and R. O. Pohl, *Rev. Mod. Phys.* **61**, 605 (1989).
- [3] J. P. Wolfe, *Imaging Phonons: Acoustic Wave Propagation in Solids* (Cambridge University Press, Cambridge, England, 1998).
- [4] V. Narayanamurti, H. L. Störmer, M. A. Chin, A. C. Gossard, and W. Wiegmann, *Phys. Rev. Lett.* **43**, 2012 (1979).
- [5] B. C. Daly, H. J. Maris, W. K. Ford, G. A. Antonelli, L. Wong, and E. Andideh, *J. Appl. Phys.* **92**, 6005 (2002).
- [6] R. M. Costescu, M. A. Wall, and D. G. Cahill, *Phys. Rev. B* **67**, 054302 (2003).
- [7] R. J. Stoner and H. J. Maris, *Phys. Rev. B* **48**, 16373 (1993).
- [8] G. Tas and H. J. Maris, *Phys. Rev. B* **55**, 1852 (1997).
- [9] P. Chen, I. V. Tomov, and P. M. Rentzepis, *J. Chem. Phys.* **104**, 10001 (1996).
- [10] C. Rose-Petruck *et al.*, *Nature (London)* **398**, 310 (1999).
- [11] A. Lindenberg *et al.*, *Phys. Rev. Lett.* **84**, 111 (2000).
- [12] D. A. Reis *et al.*, *Phys. Rev. Lett.* **86**, 3072 (2001).
- [13] M. F. DeCamp *et al.*, *Phys. Rev. Lett.* **91**, 165502 (2003).
- [14] M. F. DeCamp, D. A. Reis, D. M. Fritz, P. H. Bucksbaum, E. M. Dufresne, and R. Clarke, *J. Synchrotron Radiat.* **12**, 177 (2005).
- [15] A. Cavalleri *et al.*, *Phys. Rev. Lett.* **85**, 586 (2000).
- [16] M. Bargheer, N. Zhavoronkov, Y. Gritsai, J. C. Woo, D. S. Kim, M. Woerner, and T. Elsaesser, *Science* **306**, 1771 (2004).
- [17] P. Sondhaus, J. Larsson, M. Harbst, G. A. Naylor, A. Plech, K. Scheidt, O. Synnergren, M. Wulff, and J. S. Wark, *Phys. Rev. Lett.* **94**, 125509 (2005).
- [18] D. A. Reis, P. H. Bucksbaum, and M. F. DeCamp, *Radiat. Phys. Chem.* **70**, 605 (2004).
- [19] C. Thomsen, H. T. Grahn, H. J. Maris, and J. Tauc, *Phys. Rev. B* **34**, 4129 (1986).
- [20] B. Batterman and H. Cole, *Rev. Mod. Phys.* **36**, 681 (1964).
- [21] S. Takagi, *Acta Crystallogr.* **15**, 1311 (1962).
- [22] D. Taupin, *Bull. Soc. Fr. Mineral. Cristallogr.* **87**, 469 (1964).
- [23] D. B. McWhan, P. Hu, M. A. Chin, and V. Narayanamurti, *Phys. Rev. B* **26**, R4774 (1982).